Supporting Information

Water Soluble Iron Oxide Nanocubes with High Values of Specific Absorption Rate for Cancer Cell Hyperthermia Treatment

Pablo Guardia[1], Riccardo Di Corato[1,2], Lenaic Lartigue[3], Claire Wilhelm[3], Ana Espinosa[4], Mar Garcia-Hernandez [4], Florence Gazeau[3], Liberato Manna[1] and Teresa Pellegrino[1,2]

[1] Istituto Italiano di Tecnologia, via Morego 30, 16163 Genova, Italy

[2] National Nanotechnology Laboratory of CNR-NANO, via per Arnesano km 5, 73100 Lecce, Italy

[3] Laboratoire Matière et Systèmes Complexes (MSC), UMR 7057, CNRS and Université Paris Diderot, 10 rue Alice Domon et Léonie Duquet, 75205 Paris cedex 13, France

[4] Instituto de Ciencia de Materiales de Madrid, Consejo Superior de Investigaciones Científicas, Cantoblanco, 28049 Madrid, Spain

AUTHOR EMAIL ADDRESS (teresa.pellegrino@iit.it)

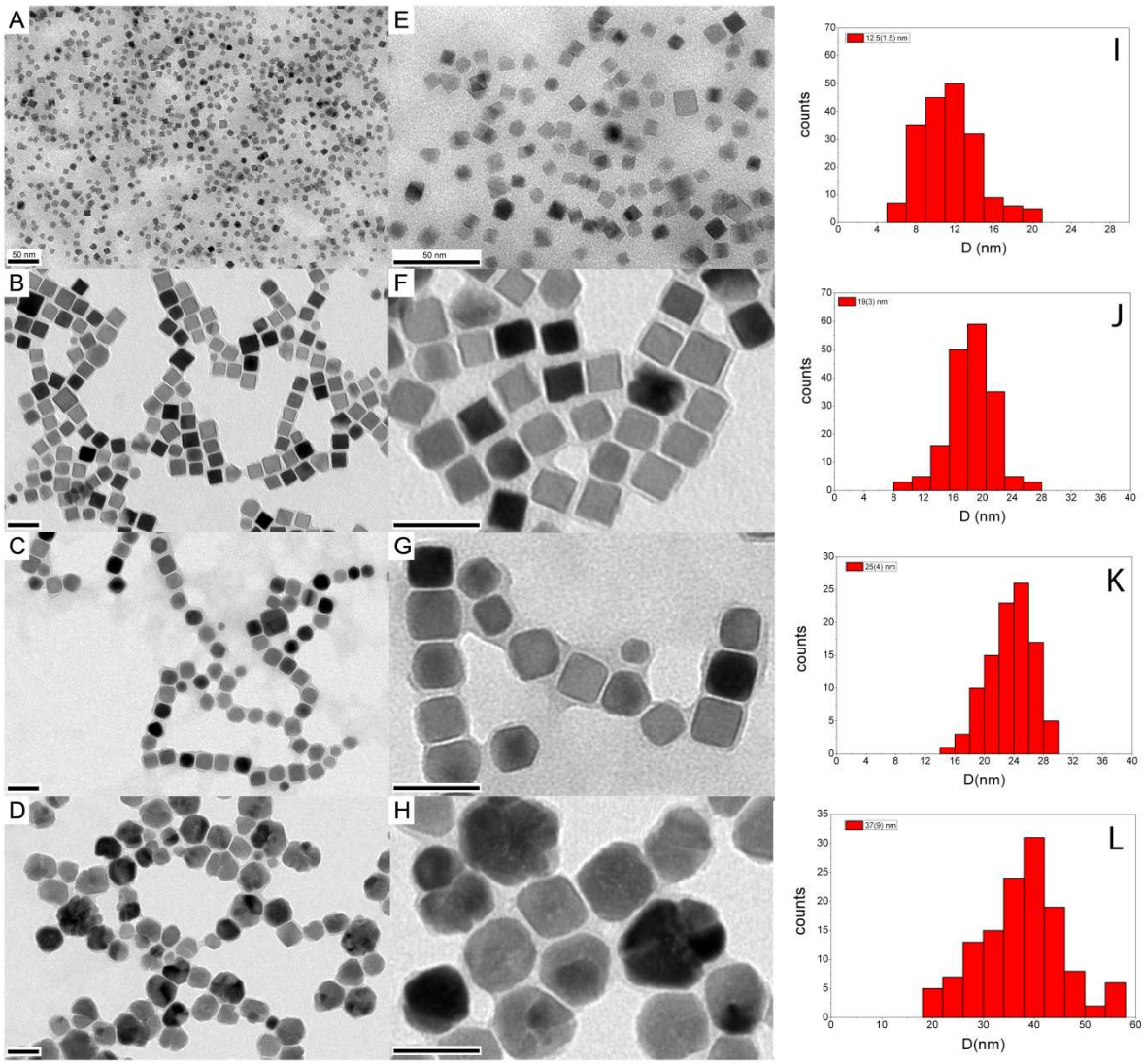

Figure S1. TEM images at low (left panels, A-D) and higher (right panels, E-H) magnification of polymer coated iron oxide nanocubes for cube-edge lengths of (A) 12 ± 1.5 nm, (B) 19 ± 3 nm , (C) 25 ± 4 nm, and (D) 38 ± 9 nm, respectively. Scale bars correspond to 50 nm for all the images. (I-L) Statistics on the TEM size of the IONCs at different cube-edge lengths.

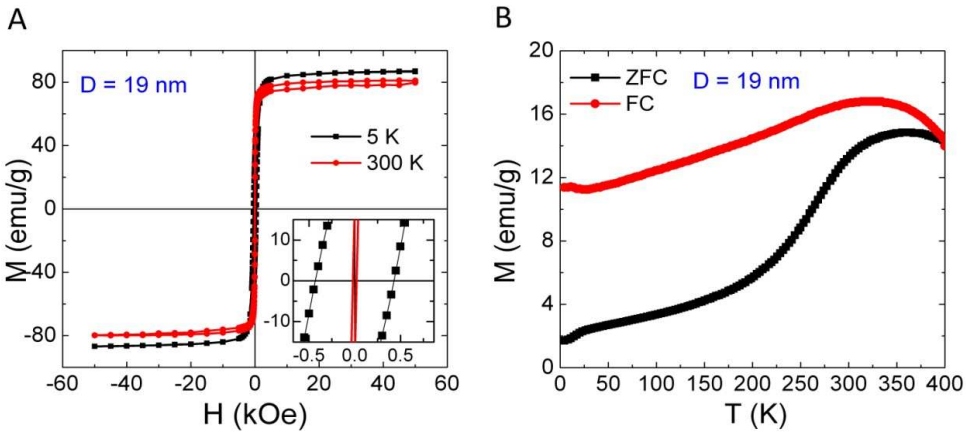

Figure S2. A) Magnetization curves at 5 K (black squares ■) and 300 K (red circles ●) and B) thermal dependence of the magnetization upon ZFC (black squares ■) and FC (red circles ●) for 19 nm IONC's performed on powder. The short distance between the magnetic dipole causes interparticle magnetic interactions which strongly affect their magnetic behavior. The onset of collective behavior of nanoparticles is clearly revealed by the shape of the FC curve. Indeed, the FC magnetization decreases as the temperature decreases below Tmax, a feature which can interpreted as the fingerprint of strong magnetostatic interparticle interactions.[1] The presence of interparticle interactions generally also induce a shift of the so-called blocking temperature T_B toward higher temperature[2, 3] To sum up, in a system of interacting nanoparticles, the maximum of ZFC curves are both influenced by the transition of superparamagnetic to ferromagnetic behavior, and the dipole-dipole interaction between each nanoparticles.

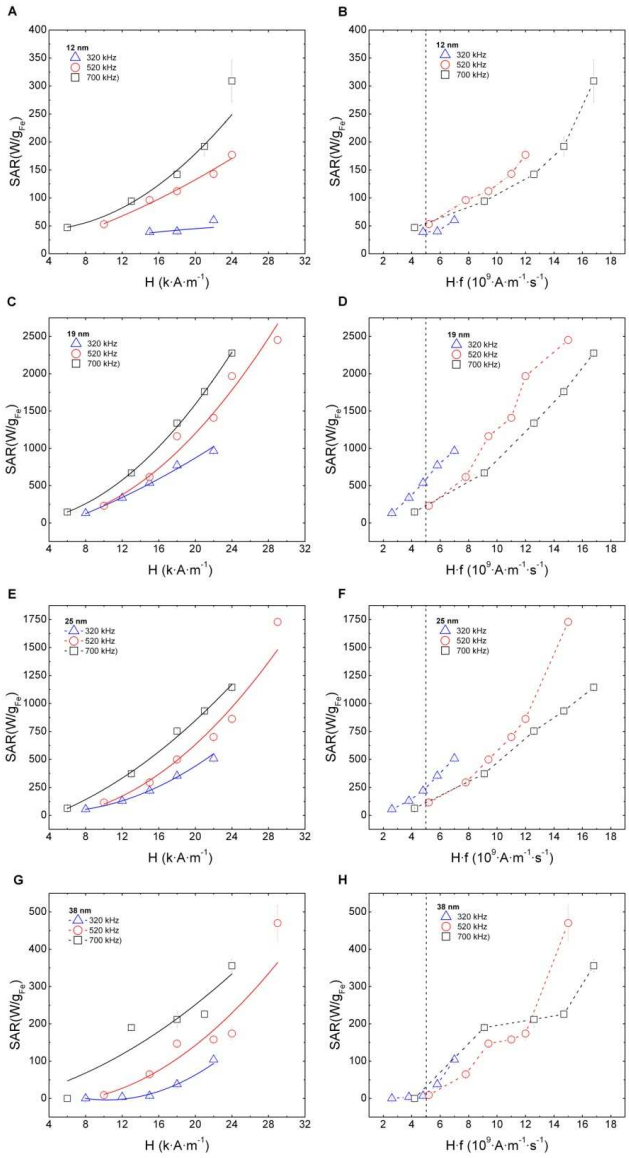

Figure S3. SAR values as a function of the applied magnetic field amplitude (right panels) and as a function of the applied magnetic field amplitude x frequency factor for (left panels) at different frequencies: 320 kHz (open blue triangles Δ), 520 kHz (open red circles ○), 700 kHz (open black squares □) for; A and B 12 nm iron oxide nanocubes, C) and D) 18 nm iron oxide nanocubes, E) and F) 25nm iron oxide nanocubes, and G) and H) 38 nm iron oxide nanocubes. The vertical dashed line defines the biological limit. Values are normalized to the iron amount per sample. Experimental data are calculated as the mean value from at least 4 measurements and error bars indicates the mean deviation. The full lines are the fits while the dashed lines are drawn as a guide to the reader.

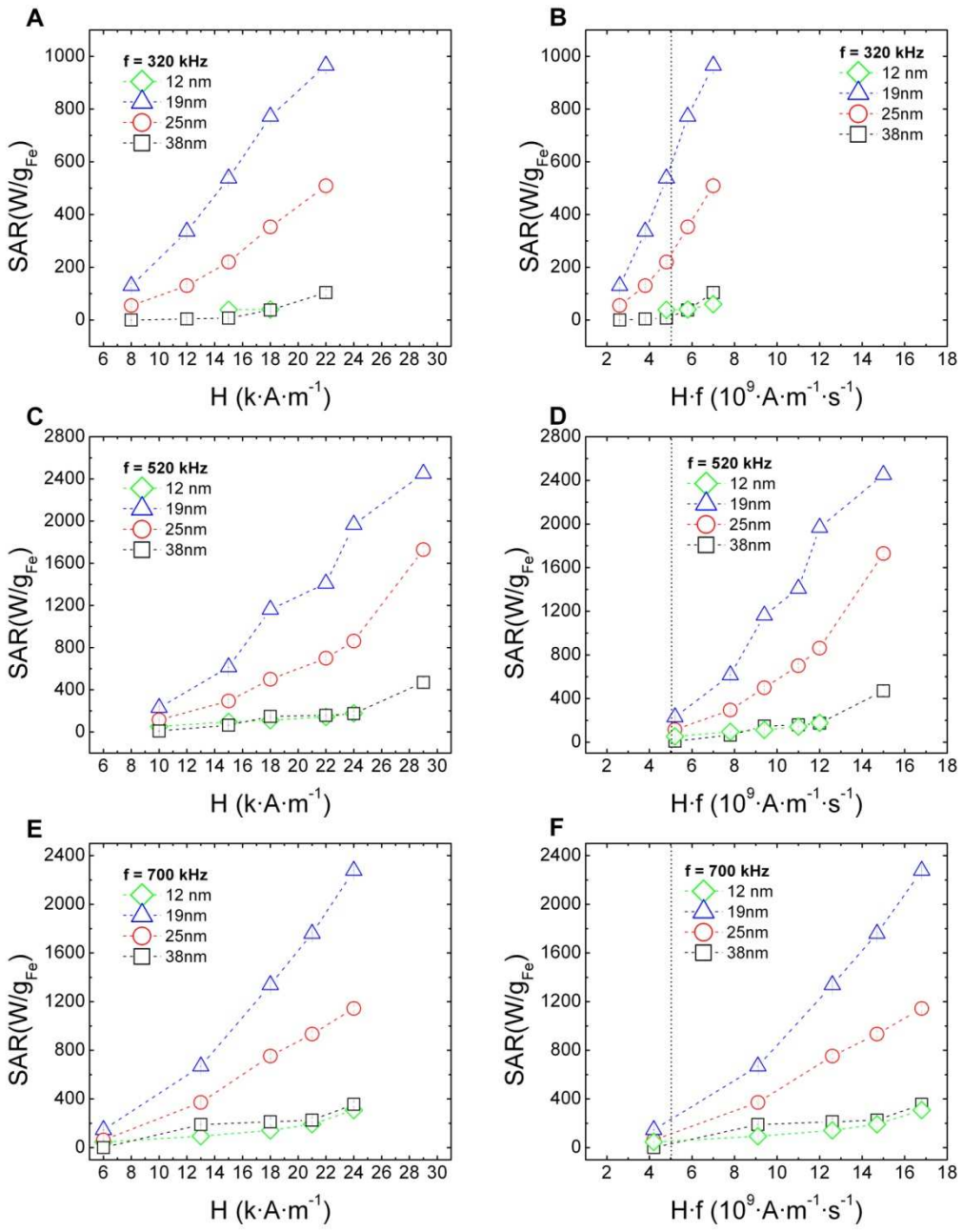

Figure S4. SAR values as a function of the applied magnetic field amplitude (left) and frequencies factor (right) for 12 nm (open green rhombs ◊) 19 nm (open blue triangles Δ), 25 nm (open red circles ○) and 38 nm (open black squares □) iron oxide nanocubes at A),B) 320 kHz, C), D) 520 kHz and E), F) 700 kHz. The black dashed line defines the biological limit. Values are normalized to the iron amount per sample. Experimental data are calculated as the mean value from at least 4 measurements and error bars indicates the mean deviation.

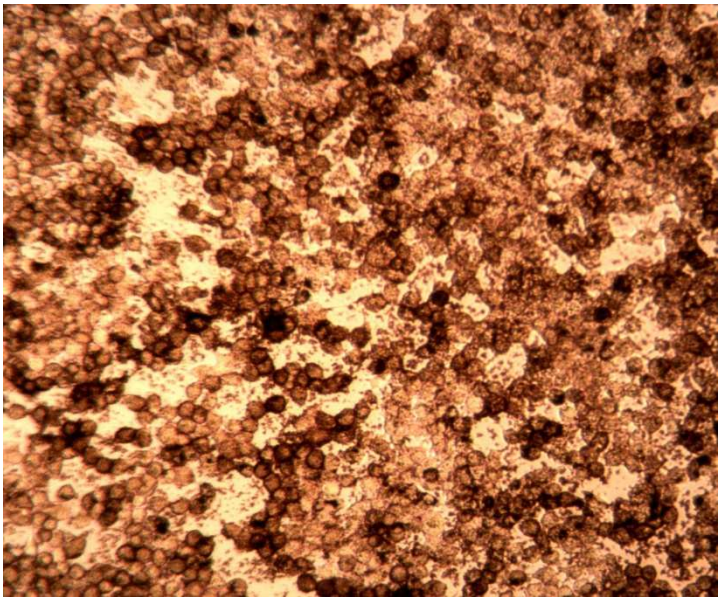

Figure S5. Optical microscope analysis of KB cells doped with IONCs-PEG for 24 hours at the concentration of 1 g/L in iron.

Appendix 1 Linear response theory

The observed square dependence of the SAR with the magnetic field and the linear dependence with the frequency are the expected behaviors predicted by the linear response theory. Such linear response theory could be still valid, when extended to larger magnetic field using the chord approximation.[4] In the approximation of randomly oriented MNPs with a strong $\sigma = K_{eff}V/k_BT$, SAR can be written as a function of the magnetic applied field as:

$$SAR = f\frac{\rho\pi\mu_0 M_S^2 V}{k_B T}.\frac{2\pi f\tau}{(1+[2\pi f\tau]^2)}H_0^2 \cong A.\tau.H_0^2$$

where $\tau = \tau_0 e^{\sigma}$, and the relaxation times and the effective anisotropy constants can be then calculated by the fitting for each of the frequency used. Note that in the calculation, nanoparticles are considered to be cubic and their relaxation to follow a pure Néel relaxation (assuming $\tau_0 = 10^{-9}$).

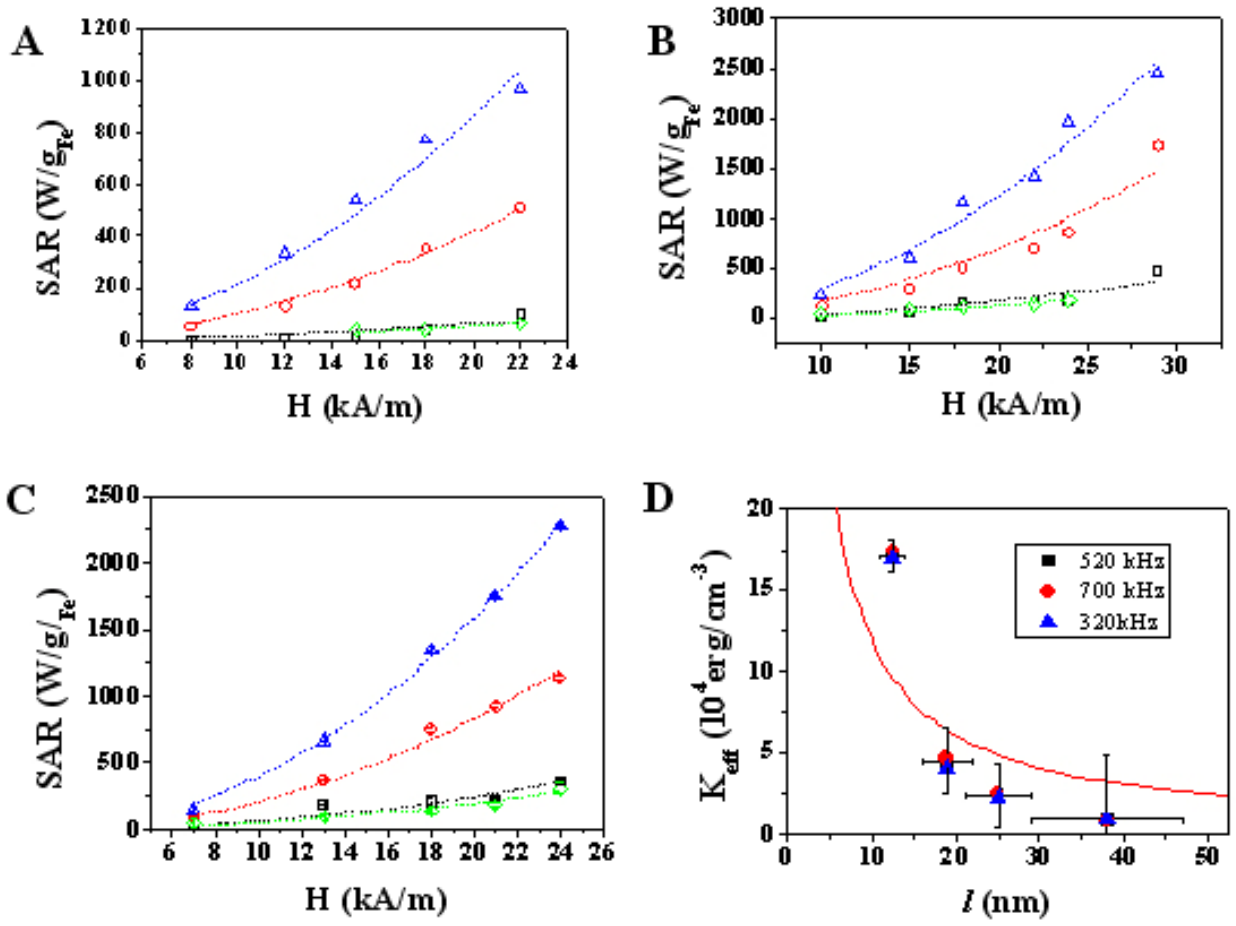

Figure S6. *SAR values as a function of magnetic field amplitude applied at a frequency of respectively: A) 320kHz, B) 520kHz and C) 700 KHz. The symbols correspond to IONPs of 12.5 ± 1.5 nm (open green rhombs ◊), 19 ± 3 nm (open blue triangles Δ), 25 ± 4 nm (open red circles ○) and 38 ±9 nm (open black squares □). Each experimental data point was calculated as the mean value of at least 4 measurements and error bars indicate the mean deviation. In each graph the dashed curves represent the fit of the SAR as a function of the magnetic field in the linear response model. D) Effective anisotropy as a function on cube edge length.*

It must be emphasized that the linear response theory remarkably fits the experimentally-found SAR values (Figure 5S, dashed lines). Moreover the anisotropy constants which are deduced from the fit do not depend on the frequency used. However it reveals an interesting behaviour of the anisotropy energy, which depends on the nanocube size, revealing a surface contribution to the effective anisotropy. Such a size dependence of the anisotropy has been observed before on α-Fe nanoparticles[5], but also on

maghemite nanoparticles synthesized by coprecipitation.[6] In the case of nanocubes, the effective anisotropy constant can be expressed as $K_{eff} = K_V + K_S/l$, where l is the edge length, K_V is the volume anisotropy and K_S the surface anisotropy. As shown in Fig.S6 D (theoretical curve in red), this expression correctly describes the values of anisotropy, taking a volume anisotropy K_V = 4.7 x 10^3 erg.cm^{-3} and an additional surface anisotropy K_S = 1 x 10^{-2} erg/cm^{-2}. The value of K_S for our cubic nanoparticles are below that found for spherical ones (K_S = 2 – 9 x 10^{-2} erg.cm^{-2}).[6-811–14] This reduction of surface anisotropy is consistent with a diminution of surface magnetic disorder in cubic-shaped nanoparticles as predicted by Salazar et al [9] In comparison with spherical nanoparticles, we also note the decrease of volume anisotropy K_V , as previously reported by Demortière et al.[10]

f = 320 kHz

Slope	Volume (m^3)	M_S (A.m^2.kg^{-1})	A*	τ
2,16E-06	**6,86E-24**	**78**	1,53E+05	1,42E-11
1,04E-06	**1,07E-23**	**83**	2,68E+05	3,88E-12
1,56E-07	**4,29E-23**	**87**	1,19E+06	1,31E-13
1,30E-07	**2,20E-24**	**65**	3,39E+04	3,83E-12

f = 520 kHz

Slope	Volume (m^3)	M_S (A.m^2.kg^{-1})	A*	τ
3,07E-06	**6,86E-24**	**78**	4,03E+05	7,62E-12
1,76E-06	**1,07E-23**	**83**	7,08E+05	2,48E-12
4,41E-07	**4,29E-23**	**87**	3,13E+06	1,41E-13
3,20E-07	**2,20E-24**	**65**	8,96E+04	3,57E-12

f = 700 kHz

Slope	Volume (m^3)	M_S ($A.m^2.kg^{-1}$)	A*	τ
3,99E-06	**6,86E-24**	**78**	7,30E+05	5,47E-12
2,08E-06	**1,07E-23**	**83**	1,28E+06	1,62E-12
6,12E-07	**4,29E-23**	**87**	5,68E+06	1,08E-13
4,94E-07	**2,20E-24**	**65**	1,62E+05	3,04E-12

References

1. Parker, D.; Dupuis, V.; Ladieu, F.; Bouchaud, J. P.; Dubois, E.; Perzynski, R.; Vincent, E., Spin-glass behavior in an interacting γ-Fe_2O_3 nanoparticle system. *Physical Review B* 2008, 77, 104428.
2. Azeggagh, M.; Kachkachi, H., Effects of dipolar interactions on the zero-field-cooled magnetization of a nanoparticle assembly. *Physical Review B* 2007, 75, 174410.
3. Lévy, M.; Gazeau, F.; Bacri, J.-C.; Wilhelm, C.; Devaud, M., Modeling magnetic nanoparticle dipole-dipole interactions inside living cells. *Physical Review B* 2011, 84, 075480.
4. Rosensweig, R. E., Heating magnetic fluid with alternating magnetic field. *Journal of Magnetism and Magnetic Materials* 2002, 252, 370-374.
5. Bødker, F.; Mørup, S.; Linderoth, S., Surface effects in metallic iron nanoparticles. *Physical Review Letters* 1994, 72, 282-285.
6. Gazeau, F.; Bacri, J. C.; Gendron, F.; Perzynski, R.; Raikher, Y. L.; Stepanov, V. I.; Dubois, E., Magnetic resonance of ferrite nanoparticles:: evidence of surface effects. *Journal of Magnetism and Magnetic Materials* 1998, 186, 175-187.
7. Tronc, E.; Ezzir, A.; Cherkaoui, R.; Chanéac, C.; Noguès, M.; Kachkachi, H.; Fiorani, D.; Testa, A. M.; Grenèche, J. M.; Jolivet, J. P., Surface-related properties of γ-Fe_2O_3 nanoparticles. *Journal of Magnetism and Magnetic Materials* 2000, 221, 63-79.
8. Dormann, J. L.; D'Orazio, F.; Lucari, F.; Tronc, E.; Prené, P.; Jolivet, J. P.; Fiorani, D.; Cherkaoui, R.; Noguès, M., Thermal variation of the relaxation time of the magnetic moment of γ-Fe_{2}O_{3} nanoparticles with interparticle interactions of various strengths. *Physical Review B* 1996, 53, 14291-14297.
9. Salazar-Alvarez, G.; Qin, J.; Sepelák, V.; Bergmann, I.; Vasilakaki, M.; Trohidou, K. N.; Ardisson, J. D.; Macedo, W. A. A.; Mikhaylova, M.; Muhammed, M.; Baró, M. D.; Nogués, J., Cubic versus Spherical Magnetic Nanoparticles: The Role of Surface Anisotropy. *Journal of the American Chemical Society* 2008, 130, 13234-13239.
10. Demortiere, A.; Panissod, P.; Pichon, B. P.; Pourroy, G.; Guillon, D.; Donnio, B.; Begin-Colin, S., Size-dependent properties of magnetic iron oxide nanocrystals. *Nanoscale* 2011, 3.